Journal of Materials Science and Engineering B 3 (7) (2013) 436-444

Effects of Stirring and Cooling on Methane Hydrate Formation in a High-Pressure Isochoric Cell

Wei Ke and Thor Martin Svartaas

Department of Petroleum Engineering, Faculty of Science and Technology, University of Stavanger, Stavanger 4036, Norway

Received: April 20, 2013 / Accepted: May 18, 2013 / Published: July 25, 2013.

Abstract: Higher mixing rates applied to hydrate-forming liquids in laboratory cell systems are commonly assumed to cause a more thorough dispersion of newly formed hydrate nuclei from gas-liquid interface into bulk liquid. There is, however, no simple and direct correlation between stirring rate and nucleation rate. Most experimental studies on hydrate kinetics in literature have been carried out at isobaric conditions. Studies in cooled systems at isochoric conditions (temperature-dependent pressures) are in scarcity. This paper presents an experimental study on effects of varying stirring rates (220-660 rpm) and varying cooling rates (0.5-10 °C/h) on the point of spontaneous nucleation (PSN) of structure-I methane hydrate. The experiments were conducted in an isochoric system with temperature and pressure both decreasing along with the continuous cooling process. Initial growth rates after nucleation were also monitored. The results suggest that higher stirring rates lead to reduced hydrate induction time and increased hydrate growth rate. The nucleation rate appeared to be slightly reduced at the lowest stirring rate (220 rpm). The degree of sub-cooling at PSN seemed to be of a more stochastic character at cooling rates lower than at 2 °C/h. Increased cooling rates trend to reduce induction time while the sub-cooling at PSN appeared to first oscillate at lower cooling rates then approach some constant level at higher cooling rates. For higher cooling rates, the nucleation rate decreased faster. Hydrate growth behavior in cooling rate experiments (0.5-10 °C/h) suggests that the total gas intake and the gas consumption rate increased with increasing cooling rate towards a constant level at 6-10 °C/h. A careful selection of stirring rate and cooling rate is essential to hydrate study.

Key words: Methane hydrate, stirring, cooling, nucleation, growth.

Nomenclature

b:	Dimensionless thermodynamic parameter
dT/dt:	Cooling rate (°C/h)
J:	Nucleation rate ($m^{-3}s^{-1}$)
K_J:	Kinetic factor ($m^{-3}s^{-1}$)
t_i:	Induction time min
T_e:	Equilibrium temperature (°C)
ΔT:	Subcooling (°C)

1. Introduction

Lab-scale hydrate formation studies [1-3] normally involve a continuous stirring and/or cooling process, helping to reduce mass and heat transfer resistances to some extent and thus create a more homogeneous environment to form hydrates. This is also considered or designed in most hydrate kinetic studies with modeling and simulation work [3-9]. A proper stirring rate and a proper cooling rate, if applied, should be carefully selected to achieve best experimental conditions for modeling work.

It is commonly assumed that it is more likely to form nuclei of super-critical size at the boundary of gas-liquid interface due to higher concentrations of both guest molecules and water. A rapid stirring could bring and disperse gas, newly formed nuclei and any pre-crystal structures from the interface to the bulk phase, making an appearance of bulk nucleation [10]. This bulk nucleation assumption prompts two straightforward questions: how does change of stirring power influence hydrate nucleation and growth respectively? Which stage of hydrate formation will stirring have a larger effect on, nucleation or growth? Wilson, et al. [11] suggested that stirring has no

---

Corresponding author: Wei Ke, research field: natural gas hydrates. E-mail: bio.kewei@gmail.com.

remarkable effect on nucleation of tetrahydrofuran (THF). Skovborg, et al. [12] reported that increased stirring would shorten the total metastable period. Bishnoi and Parent [2] claimed that stirring would flatten both temperature and composition gradients in the bulk phase, improve heat and mass transfer efficiency, and therefore give faster super-saturation and faster hydrate formation. An earlier study by Bishnoi and Vysniauskas [3] suggested that crystals tend to accumulate at gas-liquid interface under low stirring rate and thus retard mass transfer by gas diffusion and thus the overall formation rate. Svandal, et al. [13] confirmed this with phase-field theory and suggested that in this circumstance the incorporation of dissolved gas in the bulk liquid would instead become the rate limiting step. Claiming again the induction time of hydrate formation becomes shorter at higher stirring rate, Bishnoi, et al. [4] further pointed out that there is an upper limit of stirring rate, above which stirring no longer affects the formation kinetics, suggesting a complete removal of both mass and heat transfer resistance around newly formed nuclei.

Through a study on progressive nucleation under steady cooling process, Kashchiev, et al. [14] have deduced an analytical expressions for the crystallization process as a function of the continuously increasing degree of subcooling, and implicitly, as a function of time. When applying constant cooling with cooling rates in the region 0.5-3 °C/min, Koh et al. [15] found no significant effect of cooling on the hydrate nucleation temperature during nucleation experiments at constant pressure. A high cooling rate (4.5 °C/min) was also adopted by Wilson et al.[11] when studying nucleation of tetrahydrofuran (THF) with an automatic lag time apparatus (ALTA). With steady state nucleation assumption, Tsuchiyama, [16] reported that the induction time of hydrate nucleation first decreases with increasing degree of subcooling or increasing cooling rate. Further increase of subcooling or cooling rate would however lead to an increase of induction time. Uchida, et al. [17] argued with a heat-conduction-limited model that it is reasonable for higher growth rates to be observed with larger degree of subcoolings. This was also confirmed by a previous work of Sloan et al. [18] when they found that the hydrate growth rate was proportional to the degree of subcooling, suggesting that hydrate crystallization was a continuous growth process.

In this work, effects of both stirring and cooling on methane hydrate formation were examined in an isochoric cell. Hydrate nucleation and growth stages were analyzed respectively, with hydrate onset point taken as the start of growth, though it is acknowledged here that there is no obvious boundary between the two stages.

2. Experimental Methods

A lab-scale isochoric high pressure titanium cell with an inner volume of 145 mL was used to study the effects of stirring and cooling rates on methane hydrate nucleation and growth. Methane gas of scientific grade 5.5 (purity 99.9995%) was used as hydrate forming gas together with distilled water (DIW). In this work, a water volume of 10 mL and 100 mL was applied for nucleation experiments and growth experiments, respectively. The effect of molar liquid water-gas ratio on methane hydrate nucleation and growth was presented in other work by Ke et al. [19]. Real-time temperature and pressure was monitored by separate sensors, exposed directly to the inner part of the cell where the hydrate formation process took place.

A magnetic drive offers stirring power with adjustable stirring rate from 0 to over 1,000 rpm. In this work, stirring rates of 220, 440 or 660 rpm were applied. A similar 3C system (closed, constant volume, continuous cooling) was applied in this work, as used by Svartaas and Fadnes [20] for their studies on methane hydrate equilibrium dissociation conditions in methane, DIW system with and without thermodynamic inhibitors present. In their studies, the temperature gradient was kept constant with a very low rate of 0.3 °C/h during the formation and dissociation cycles. However, they focused their study on the final hydrate dissociation points where low heating rate is required to maintain system at local equilibrium throughout the dissociation process. Higher cooling rates were applied in this work. A programmable refrigerated and heating circulator produced desired cooling rates of 0.5, 2, 6 and 10 °C/h.

A detailed description of experimental setup and experimental procedure could be found in another work by Ke et al. [21], where they investigated kinetic hydrate inhibitors in a similar hydrate-forming system.

3. Results

3.1 Effect of Stirring on Hydrate Formation

Measured effects of stirring rates on induction time and subcooling at point of spontaneous methane hydrate nucleation (PSN) are given in Table 1. The average values ±SD were based on a total number of 10 parallel experiments for each dataset. During all experiments other conditions such as water/gas ratio, cooling rate, initial P and T conditions at start of experiments were kept constant (10 mL DIW + 135 mL methane gas, 6 °C/h, 90.5 bar, 14.1 °C, respectively).

Table 1 Results of nucleation tests with varying stirring rates.

Stirring rate (rpm)	Induction time (min)	Subcooling (°C)
220	49.0 ± 5.7	4.6 ± 0.6
440	37.3 ± 6.8	3.6 ± 0.7
660	39.5 ± 4.3	3.8 ± 0.4

At constant cooling rate, dT/dt (6 °C/h), induction time t_i is linearly related to the degree of subcooling, ΔT, as given by Eq. (1):

$$t_i = \frac{\Delta T}{dT/dt} \tag{1}$$

Fig. 1 shows average degree of subcooling ±SD (standard deviation) at the different stirring rates examined. Taking the ±SD into consideration all induction times and sub-cooling values are within overlapping regions and are thus not significantly different. The stippled curve (cubic spline fit) in Fig. 1 should thus only be taken as illustrative.

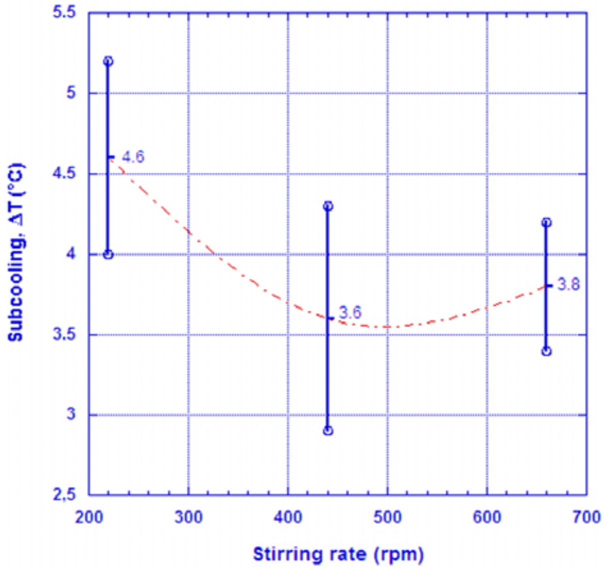

Fig. 1 Degree of subcooling with varying stirring rates. The stippled curve is based on cubic spline fit of the average ΔT.

As described in the other paper by Ke, et al. [21], the model by Kashchiev, et al. [14] for calculating time-dependent average nucleation rate, J ($m^{-3}\cdot s^{-1}$), as given by Eq. (2), was applied in the present work:

$$J = K_J \exp[-b/(1-\Delta T/T_e)(\Delta T/T_e)^2] \tag{2}$$

With continuous cooling, T_e and ΔT in Eq. (2) refer to the equilibrium temperature and time dependent degree of sub-cooling at experimental pressure, respectively. $\Delta T/T_e$ is a relative degree of sub-cooling. Eq. (2) above also involves a kinetic factor, K_J ($m^{-3}\cdot s^{-1}$), and a dimensionless thermodynamic parameter, b. The kinetic factor K_J and the thermodynamic parameter b in Eq. (2) were set to be 1.00E + 21 $m^{-3}\cdot s^{-1}$ and 0.38 for cubic nuclei respectively. The feasibility of applying Eq. (2) with a further explanation on the use of parameters K_J and b were explained by Ke, et al. [21].

Based on this model, the average nucleation rate at the different stirring rate applied was calculated along the cooling process for the last 10 min prior to point of spontaneous nucleation (PSN), as shown in Fig. 2. The time elapsed before hydrate onset was negative since the onset point was defined as time zero for the process.

From Table 1 and Figs. 1 and 2, it can be seen that a reduction of the stirring rate from 660 rpm to 220 rpm, the induction time t_i and degree of sub-cooling, ΔT at PSN both increased slightly, while the average nucleation rate during the last 10 min prior to PSN decreased. This observation was consistent with the theory that higher stirring rate helps bring and disperse newly formed hydrate nuclei from gas-liquid interface into bulk liquid phase. Higher stirring rate also helps reduce mass and heat transfer resistance around all newly formed hydrate nuclei. 440 rpm stirring rate apparently caused reduced induction time than observed at 660 rpm, though not significantly different. Similarly the average nucleation rate during the last 10 min prior to PSN appeared to be slightly higher at 440 rpm than at 660 rpm. Recall theories mentioned in the Introduction section on effect of physical agitation on hydrate nucleation, some researchers claimed that there was an upper limit of stirring rate above which higher stirring rate would no longer affect the nucleation kinetics [4]. This helps explain the close results from 440 rpm and 660 rpm experiments. In the present work, it was assumed that the effect of physical stirring power on hydrate nucleation is a struggling balance between nuclei/nuclei size distribution in the bulk phase and a contribution to progressive nuclei growth. Only a stirring rate that can (1) maximize its efficiency to distribute the newly and continuously forming nuclei into a whole bulk phase and (2) reduce mass and heat transfer resistance while at the same time not retard the progressive nuclei growth (by means of generating fluid turbulence for example), could be considered a most appropriate stirring rate. In this sense, 440 and 660 rpm could be deemed as both appropriate to promote nucleation in this case, with a trend that an even higher stirring rate would probably no longer be applicable.

Analyzing growth rates over a 20 min period after PSN and nucleation rates during the last 10 min prior to PSN, a total hydrate formation time of 30 min was analyzed in the present study. This time period is deemed long enough to acquire data and knowledge on hydrate nucleation and growth. It also applies to the following work in this paper regarding the effect of cooling on methane hydrate formation.

Growth results at the examined stirring rates are given in Table 2. All growth experiments were conducted in excess water system using 100 mL DIW + 45 mL methane gas at a constant cooling rate of 6 °C/h.

Figs. 3 and 4 show time-dependent gas consumption (in bar) and gas consumption rate (in bar/min) at the different stirring rates applied. A pseudo-steady-state approximation [10] was made, assuming that at any time the rate of gas consumed by growing hydrate equals the rate of gas consumed from

Table 2 Measured and calculated growth data obtained within the first 20 min after hydrate onset at the examined stirring rates.

Stirring rate (rpm)	Total gas intake (bar)	Initial growth rate (bar/min)	Average growth rate (bar/min)
220	3.2	0.11	0.16
440	12.5	0.47	0.63
660	19.2	0.83	0.96

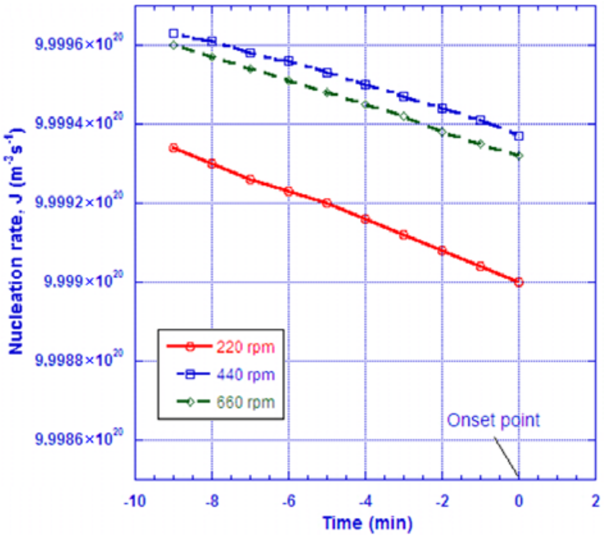

Fig. 2 Average nucleation rate, J(m^{-3}s^{-1}) for the last 10 min before hydrate onset point in stirring rate tests.

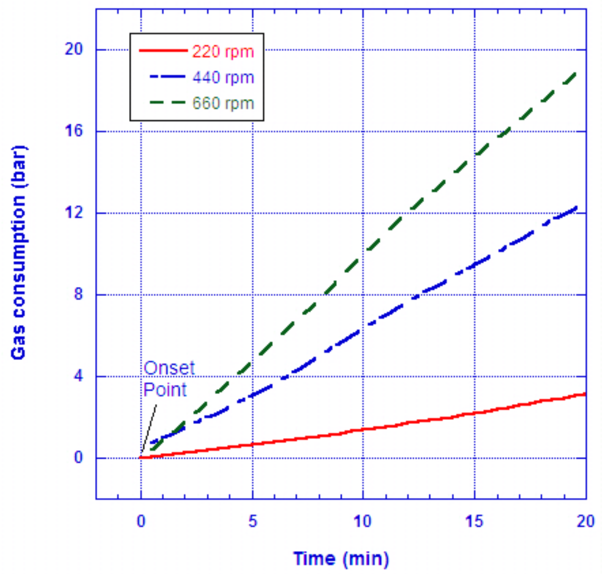

Fig. 3 Gas consumption as function of time at the stirring rates examined.

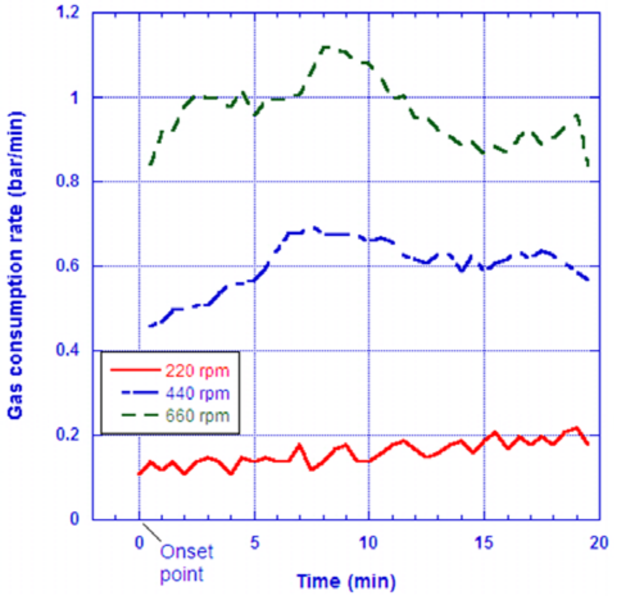

Fig. 4 Gas consumption rate during the first 20 min after hydrate onset at the different stirring rates applied.

the gas phase. It is not always proper to apply this assumption. A representative circumstance would be that if system temperature undergoes very fast change, the resulting change of gas solubility in the bulk liquid phase may lead to a sufficient difference in gas consumption rate and hydrate growth rate. For simplicity, the gas consumption rate as measured directly from experimental pressure drop due to hydrate formation was equivalently taken as hydrate growth rate in this work. In these calculations the baseline pressure was estimated from PT relation in system prior to hydrate formation.

Figs. 5 and 6 show the total gas intake (bar) and the initial and average growth rate (bar/min) respectively.

As seen from Table 2 and Figs. 3-6, total gas intake, initial hydrate growth rate and average growth rate increased with increasing stirring rate during the first 20 min after hydrate onset. The increases are apparently linear functions of stirring rate over the range of stirring rates examined.

A higher stirring rate promoted remarkably the hydrate growth at an early stage of catastrophic hydrate formation, as shown in Fig. 3. It is also seen from Fig. 4 that the smooth and progressive methane hydrate formation held true at all varying stirring rates, at around a stable speed, respectively, from approximately 0.2-1 bar/min. With experimental studies on methane and ethane hydrate formation,

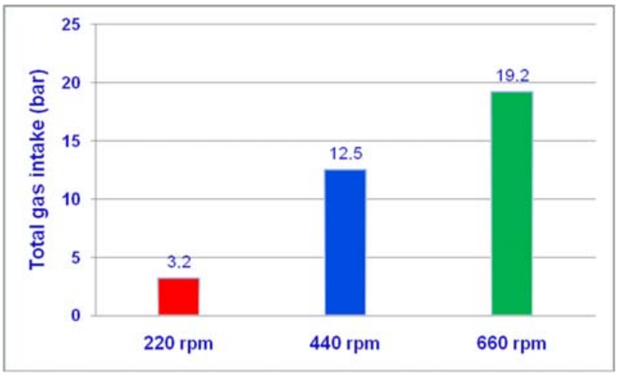

Fig. 5 Total gas intake at examined stirring rates within the first 20 min after hydrate.

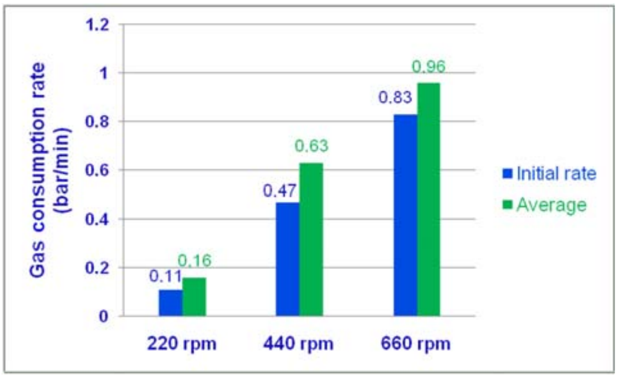

Fig. 6 Graph showing the initial and average gas consumption rate during the first 20 min after hydrate onset at the examined stirring rates.

Skovborg and Rasmussen [22] also reported a similar hydrate growing behavior with an almost constant growth rate. They assumed that the transport of gas molecules from gas phase to bulk liquid phase was the rate limiting step for hydrate growth. If this gas transport process is stable, a constant and stable growth rate could also be expected.

A comparison with previous nucleation results [4, 10-13] of stirring rate experiments suggested that although a higher stirring rate does not necessarily promote hydrate nucleation, it does promote hydrate growth in a more predictable manner. This could be most probably due to the fact that a high stirring rate helps improve gas diffusion from gas phase into the bulk liquid phase and also increase the total contact area for hydrate nuclei to grow with more sufficient gas and water supply during the time period of 20 min for comparison. Considering effects of stirring on both methane hydrate nucleation and growth, 660 rpm was considered to be the most suitable stirring rate for promotion of methane hydrate formation and thus taken as a default stirring rate in further studies.

3.2 Effect of Cooling on Hydrate Formation

Table 3 shows measured effects on nucleation as function of cooling rate. The average values ±SD were based on a total number of 10 parallel experiments for each dataset. During all experiments other conditions such as water/gas ratio, stirring rate and the initial P and T conditions at start of experiments were kept constant (10 mL water + 135 mL methane gas, 750 rpm, 90.5 bar, 14.1 °C, respectively).

Fig. 7 shows the sub-cooling as function of cooling rate.

Similar to the analysis on effects of stirring rate, the effect of cooling rate on the average nucleation rate was calculated for the last 10 min before hydrate onset, as shown in Fig. 8. Time before the onset point was negative since onset point was defined as time zero for the process.

Table 3 Results of nucleation experiments as function of varying cooling rates.

Cooling rate (°C/h)	Induction time (min)	Subcooling (°C)
0.5	306.3 ± 81.3	2.5 ± 0.7
2	60.7 ± 8.7	2.0 ± 0.3
6	39.5 ± 4.3	3.8 ± 0.4
10	45.0 ± 14.2	4.2 ± 0.7

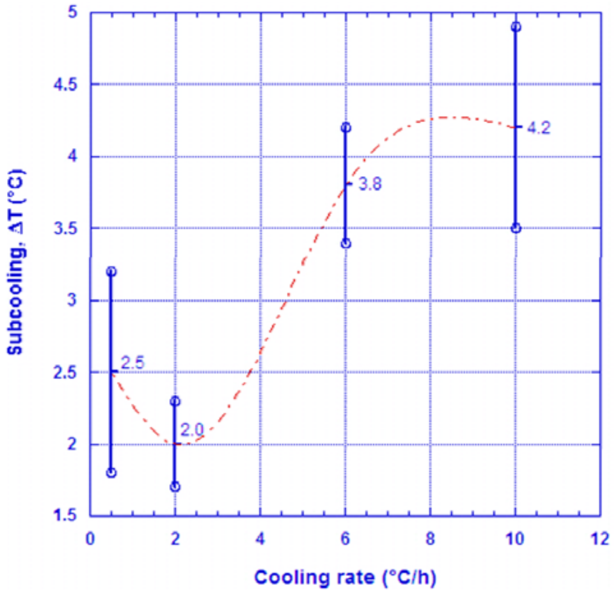

Fig. 7 Degree of subcooling with varying cooling rates.

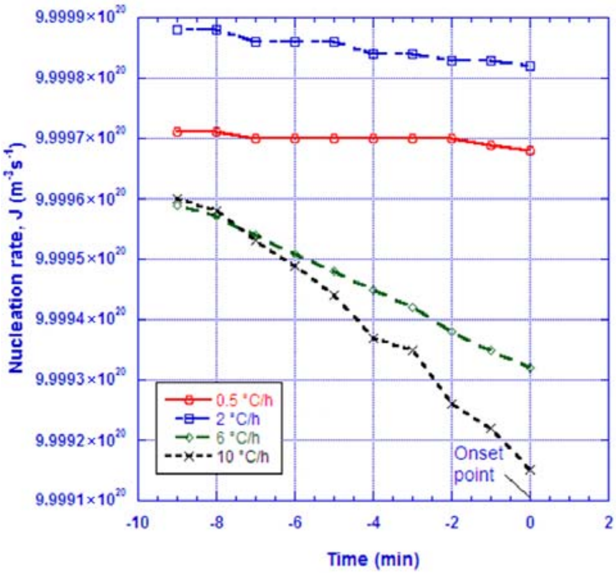

Fig. 8 Average nucleation rate, J($m^{-3}s^{-1}$) for the last 10 min before hydrate onset in cooling rate tests.

Koh et al.[15] and Wilson et al. [11] applied very high cooling rates of up to a few °C per minute and found no remarkable effect of cooling on the hydrate nucleation temperature. As seen from Table 3 and

Figs. 7 and 8, effect of cooling rate on nucleation was observed when slower rates in the region around a few degrees per hour are applied. When the cooling rate increased from 0.5 °C/h to 2 °C/h the induction time and degree of sub-cooling decreased from 306 min and 2.5 °C to 61 min and 2.5 °C in average respectively. At the higher cooling rates (6 and 10 °C/h), the degree of sub-cooling at onset of hydrate formation appeared to approach a slightly higher and constant level. This observation was consistent with observations by Uchida, et al. [17].

Considering hydrate formation as a continuous crystallization process, as Kashchiev, et al. [14] have pointed out, the nucleation rate of newly forming nuclei in the bulk liquid phase would be a function of the continuously increasing degree of sub-cooling. The reason why other factors and experimental parameters, typically the pressure, need not to be considered with effect on nucleation and nucleation rate is that, during the time period of 10 min before spontaneous growth the system pressure was kept almost constant. As shown by Fig. 8 the initial nucleation rates observed 10 min prior to onset of hydrate formation were all close to 1.0 × 10^{21} $m^{-3}s^{-1}$ for all cooling rates examined. For the two lowest cooling rates (0.5 and 2 °C/h) the nucleation rates were nearly constant over the 10 min period. The higher cooling rates (6 and 10 °C/h) gave a pronounced decreasing rate due to increasing sub-cooling during the same period of analysis.

Measured growth rates as function of cooling rate during the first 20 min after hydrate onset are given in Table 4. The experiments were conducted at fixed stirring rate (660 rpm) and with excess water in cell (100 mL water + 45 mL methane at 90 bars).

Table 4 Growth rates measured at different cooling rates during the first 20 min after hydrate onset.

Cooling rate (°C/h)	Total gas intake (bar)	Initial growth rate (bar/min)	Average growth rate (bar/min)
0.5	6.9	0.42	0.36
2	11.2	0.68	0.56
6	19.2	0.83	0.96
10	18.8	0.75	0.94

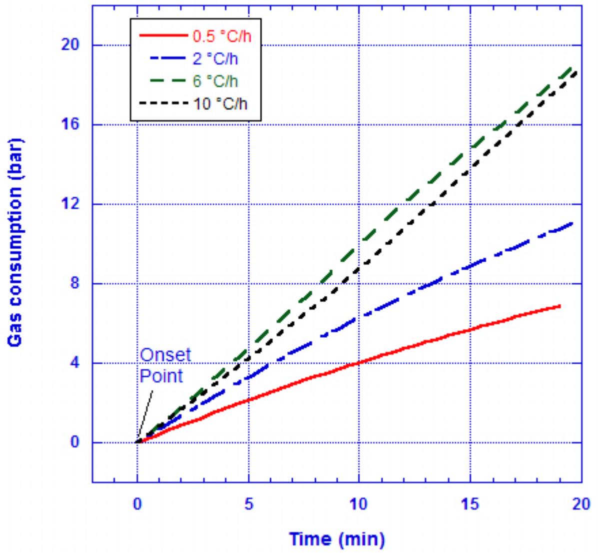

Fig. 9 Gas consumption with time in cooling rate experiments (20 min after hydrate onset).

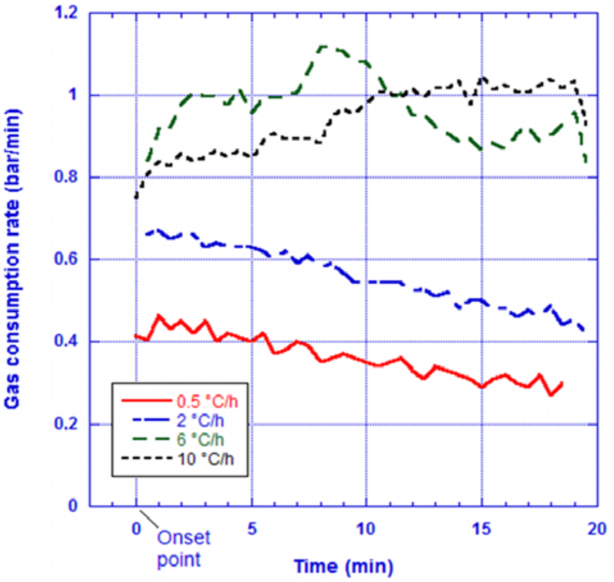

Fig. 10 Gas consumption rate in cooling rate experiments (20 min after hydrate onset).

During the growth experiment at cooling rate of 0.5 °C/h the data sampling was interrupted for a short period of time at 19 min due to logger failure. For this experiment the total gas intake, initial growth rate and average growth rate were all based on the first 19 min after hydrate onset. Figs. 9 and 10 show time-dependent gas consumption (in bar) and gas consumption rate (in bar/min) at the different cooling rates examined. The gas consumption rate was measured directly from experimental pressure drop, and was taken equivalently as hydrate growth rate. (PT relation of system without hydrates was used as baseline for calculation of pressure drop due to hydrate formation.)

Figs. 11 and 12 show total gas intake (bar) and initial and average growth rate (bar/min) respectively.

As seen from Table 4 and Figs. 9 to 12, total gas intake, initial hydrate growth rate and average growth rate during the first 20 min after hydrate onset were all increasing as function of increasing cooling rate up to some threshold level which was reached at a cooling rate around 6 °C/h. Within a same growth period of time, the total accumulated degree of subcooling was proportional to the cooling rate and thus it was reasonable to assume that the growth rate would increase in proportion to the increase of cooling rate. This result further indicates that the hydrate growth is a continuous crystallization process, with growth kinetics largely controlled by the degree of subcooling. Meanwhile, with very close results from 6 °C/h and 10 °C/h, it is also seen that the hydrate growth rate was reaching a threshold level for cooling rates above 6 °C/h. Recall the behavior of increasing stirring rates in previous study, as shown in Table 2 and Figs. 3-6, the hydrate formation kinetics is apparently no longer affected by cooling rate above an upper limit. In our case, this limit could be around 6 °C/h.

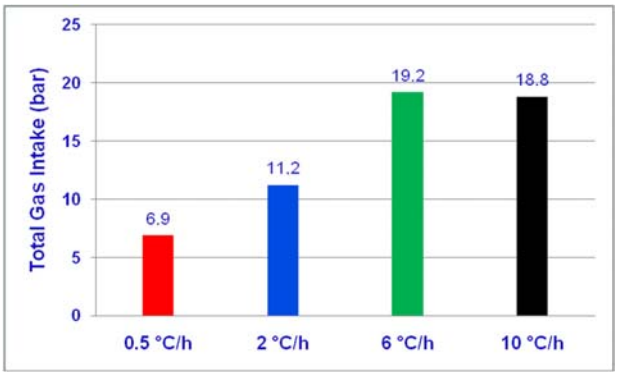

Fig. 11 Total gas intake under varying cooling rates within the first 20 min after hydrate onset.

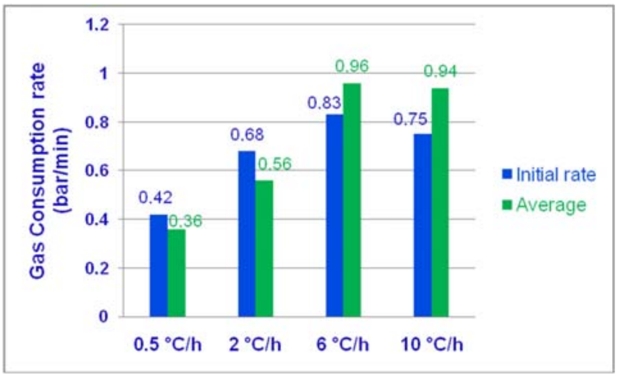

Fig. 12 Initial and average gas consumption rate at varying cooling rates within the first 20 min after hydrate onset.

Combining information gained from Table 3 and Figs. 7 and 8, it was seen that the effect of cooling on methane hydrate nucleation oscillated at lower cooling rates. As a comparison, the way how application of cooling influences hydrate growth, as shown in this study, seems to be more regular and predictable.

4. Conclusions

This paper has presented an experimental study on the effects of stirring and cooling on methane hydrate nucleation and growth in isochoric cell experiments. The effect of stirring on hydrate nucleation is taken as a balance of nuclei/nuclei size distribution in the bulk phase and a contribution to progressive nuclei growth. Meanwhile, increasing stirring rate would increase total gas consumption and hydrate growth rate. For hydrate formation it is necessary to choose an appropriate stirring rate considering its effects on both nucleation and growth. The effect of cooling on methane hydrate nucleation oscillated slightly at lower cooling rates, while higher cooling rates promoted hydrate growth to a seemingly saturated level. Hydrate nucleation is stochastic, while hydrate growth is a continuous crystallization process. An appropriate stirring rate and cooling rate should be carefully chosen for specific hydrate studies.

Acknowledgments

The authors thank the Ministry of Education and Research of Norway (Kunnskaps Departementet) and the University of Stavanger for the financial support

of this work.

References

[1] D. Kashchiev, A. Firoozabadi, Nucleation of gas hydrates, Journal of Crystal Growth 243 (2002) 476-489.

[2] J.S. Parent, P.R. Bishnoi, Investigations into the nucleation behavior of methane gas hydrates, Chem. Eng. Comm 144 (1996) 51-64.

[3] A. Vysniauskas, P.R. Bishnoi, A kinetic study of methane hydrate formation, Chemical Engineering Science 38 (1983) 1061-1072.

[4] P. Englezos, N. Kalogerakis, P.D. Dholabhai, P.R. Bishnoi, Kinetics of formation of methane and ethane gas hydrates, Chemical Engineering Science 42 (1987) 2647-2658.

[5] P. Englezos, Kinetics of gas hydrate formation and kinetic inhibition in offshore oil and gas operations, in: Proceedings of the 5th International Offshore and Polar Engineering Conference, Hague, Netherlands, (1995) 289-296.

[6] K. Lekvam, P. Ruoff, A reaction kinetic mechanism for methane hydrate formation in liquid water, J. Am. Chem. Soc 115 (1993) 8565-8569.

[7] RW. Hawtin, C. Moon, P.M. Rodger, Simulation of hydrate kinetic inhibitors: The next level, in: Proceedings of the 5th International Conference on Gas Hydrates, Trondheim, Norway, 2005.

[8] C. Moon, R.W. Hawtin, P.M. Rodger, Direct molecular simulations of hydrate nucleation, in: Proceedings of the 5th International Conference on Gas Hydrates, Trondheim, Norway, 2005.

[9] J.C. Ribeiro, P.L.C. Lage, Modelling of hydrate formation kinetics: state-of-the-art and future directions, Chemical Engineering Science 63 (2008) 2007-2034.

[10] E.D. Sloan, C.A. Koh, Clathrate Hydrates of Natural Gases, 3rd ed., CRC Press/Tayler & Francis, Boca Raton, FL, 2008, p. 130.

[11] P.W. Wilson, D. Lester, A.D.J. Haymet, Heterogeneous nucleation of clathrates from supercooled tetrahydrofuran (THF)/water mixtures, in: Proceedings of the 5th International Conference on Gas Hydrates, Trondheim, Norway, 2005.

[12] P. Skovborg, H.J. Ng, P. Rasmussen, U. Mohn, Measurement of induction times for the formation of methane and ethane gas hydrates, Chemical Engineering Science 48 (1993) 445-453.

[13] A. Svandal, B. Kvamme, L. Granasy, T. Pusztai, T. Buanes, J. Hove, The phase-field theory applied to CO_2 and CH_4 hydrate, Journal of Crystal Growth 287 (2006) 486-490.

[14] D. Kashchiev, A. Borissova, R.B. Hammond, K.J. Roberts, Effect of cooling rate on the critical undercooling for crystallization, Journal of Crystal Growth 312 (2010) 698-704.

[15] K.C. Hester, S.R. Davies, J.W. Lachance, E.D. Sloan, C.A. Koh, Hydrate nucleation measurements using high pressure differential scanning calorimetry, in: Proceedings of the 6th International Conference on Gas Hydrates, Vancouver, Canada, 2008.

[16] A. Tsuchiyama, Crystallization kinetics in the system $CaMgSi_2O_6$-$CaAl_2Si_2O_8$: the delay in nucleation of diopside and anorthite, American Mineralogist 68 (1983) 687-698.

[17] T. Uchida, I.Y. Ikeda, S. Takeya, T. Ebinuma, J. Nagao, H. Narita, CO_2 hydrate film formation at the boundary between CO_2 and water: Effects of temperature, pressure and additives on the formation rate, Journal of Crystal Growth 237-239 (2002) 383-387.

[18] E.M. Freer, M.S. Selim, E.D. Sloan, Methane hydrate film growth kinetics, Fluid Phase Equilibria 185 (2001) 65-75.

[19] W. Ke, T.M. Svartaas, The effect of molar liquid water-gas ratio on methane hydrate formation, in: Proceedings of the 7th International Conference on Gas Hydrates, Edinburgh, Scotland, United Kingdom, 2011.

[20] T.M. Svartaas, F.H. Fadnes, Methane hydrate equilibrium data for the methane-water-methanol system up to 500 bara, in: Proceedings of the 2nd International Offshore and Polar Engineering Conference, San Francisco, USA, 1992, pp.614-619.

[21] W. Ke, T.M. Svartaas, H.K. Abay, Effects of low concentration methanol, PVP and PVCap on structure-I methane hydrate formation, Journal of Energy and Power Engineering 7 (2013) 432-439.

[22] P. Skovborg, P. Rasmussen, A mass transport limited model for the growth of methane and ethane gas hydrates, Chemical Engineering Science 49 (1994) 1131-1143.